https://doi.org/10.5194/egusphere-2024-565
Preprint. Discussion started: 21 March 2024

Predicting the Risk of Glacial Lake Outburst Floods in Karakorum

Nazir Ahmed Bazai [1,2], Paul A. Carling [3*], Peng Cui [2,4*], Hao Wang [2,4], Zhang Guotao [4], Liu Dingzhu [4,5,6], Javed Hassan [7]

[1] Key Laboratory of Mountain Hazards and Earth Surface Process/Institute of Mountain Hazards and Environment, Chinese Academy of Sciences (CAS), Chengdu, China
[2] China-Pakistan Joint Research Center on Earth Sciences, Chinese Academy of Sciences and HEC, Islamabad, Pakistan.
[3] Geography and Environmental Science, University of Southampton, Southampton SO17 1BJ, UK
[4] Institute of Geographic Sciences and Natural Resources Research, Chinese Academy of Sciences, Beijing, China
[5] Earth Surface Process Modelling, German Research Centre for Geosciences (GFZ), Potsdam, Germany
[6] National Disaster Reduction Centre of China, Ministry of Emergency Management, Beijing, China
[7] DTU Space, Technical University of Denmark, 2800 Kongens Lyngby, Denmark

Correspondence to: Paul A. Carling: p.a.carling@soton.ac.uk and Peng Cui: pengcui@imde.ac.cn

Abstract. Glacier snouts respond to climate change by forming proglacial meltwater lakes, thereby influencing glacier mass balance and leading to advancements and surges. The positive feedback of climate change results in more frequent ice-dammed glacial lake outburst floods (GLOFs) in the Karakorum and surrounding regions, often facilitated by englacial conduits. However, the complex and multi-factor processes of conduit development are challenging to measure. Determining the lake depths that might trigger GLOFs and the numerical model specifications for breaching are still being determined. Empirical estimates of lake volumes, along with field-based monitoring of lake levels and depths and the assessment of GLOF risks, enable warnings and damage mitigation. Using historical data, remote sensing techniques, high-resolution imagery, cross-correlation feature-tracking, and field-based data, we identified the processes of lake formation, drainage timing, and triggering depth. We developed empirical approaches to determine lake volume and trigger water pressure leading to a GLOF. The correlation of glacier surge and lake volume reveals that glacier surge velocity plays a crucial role in lake formation and controlling the size and volume of the lake. Lake volume estimation involves geometric considerations of the lake basin shape. A GLOF becomes likely when the lake's non-dimensional depth (n') exceeds 0.60, correlating with a typical water pressure on the dam face of 510 kPa. Additionally, we identified the critical risk zone of lakes, where all lake outburst floods occur, as the point where the lake volume reaches or exceeds 60% of its capacity. These field-based and empirical findings not only offer valuable insights for early warning procedures in the Karakorum but also suggest that similar approaches can be effectively applied to other mountain environments worldwide where GLOFs pose a hazard.

1. Introduction

Globally, glacier shrinkage is a strikingly visible sign of climate change. However, within High Mountain Asia (HMA), particularly the Karakorum, Kunlun Shan, and Eastern Pamirs, the glaciers have been gaining mass since 1970 (Berthier and Brun, 2019; Gardelle et al., 2012; Kääb et al., 2015; Minora et al., 2013; Yao et al., 2012). This positive response to climate change consequently influences glacier dynamic behaviours, with the HMA glaciers thickening, increasing glacier surges, and

https://doi.org/10.5194/egusphere-2024-565
Preprint. Discussion started: 21 March 2024

advancing glacier termini throughout the region (Bhambri et al., 2013; Bolch et al., 2017). This behaviour contrasts neighbouring regions with negative glacier mass budgets, such as the Himalayas, Hindukush, and Tibet (Bazai et al., 2021; Bolch et al., 2011; Frey et al., 2014). In the latter areas, glaciers continue to shrink, thinning and reducing volume, showing no significant glacier advance (Dehecq et al., 2019; Farinotti et al., 2020; Yao et al., 2012). As a result, the Moraine Lake formation has increased the number of GLOFs in the glacier-retreating regions (Yong et al., 2017) as well as the number of glacier avalanches as increased (Byers et al., 2023; Kääb and Girod, 2023; You and Xu, 2022). However, in the glacier advance regions, the positive variation in regional climate feedback has prompted the rapid formation of ice-dammed lakes accompanied by sudden releases of meltwater originating from these lakes (Carling, 2013; Hewitt, 1982; Hewitt, 1998; Hewitt and Liu, 2010).

The mechanisms and frequency of ice dam glacial lake outburst floods (GLOFs) still need to be better understood, hindering accurate prediction (Bazai et al., 2021; Cook et al., 2016; Harrison et al., 2018; Richardson and Reynolds, 2000). Recent studies have investigated changes in frequency due to climate change (Rick et al., 2023; Veh et al., 2023) and conducted global assessments of flood volume and risk (Rick et al., 2023). Despite these efforts, understanding the drainage and predicting flood events from ice-dammed lakes remain challenging. Predicting these events is crucial due to their potential to cause devastating impacts on human lives and livelihoods, ecosystems, infrastructure (*e.g.*, roads, bridges, hydropower systems), river channel stability, and effects on agriculture and fisheries (Carrivick and Tweed, 2016; Cook et al., 2016; Emmer, 2017; John et al., 2000; Neupane et al., 2019; Zhang et al., 2022).

Ice-dammed Lake floods represent the dominant hazard in cryospheric regions, comprising 70% of GLOFs. In contrast, moraine-dammed lakes contribute only 9% (with the remaining 16%, 3%, and 2 % triggered by unknown dam types, volcanic activity, and bedrock, respectively) (Carrivick and Tweed, 2016). GLOFs have been recorded causing damage up to 120 km from moraine-dammed lakes (Richardson and Reynolds, 2000) and around 500 km from ice-dammed lakes (Hewitt and Liu, 2010). The resulting impacts include hundreds of human fatalities and the other impacts noted above (Carrivick and Tweed, 2016; Cui et al., 2014; Cui et al., 2015; Kreutzmann, 1994; Mason, 1929; Stuart-Smith et al., 2021; Zhang, 1990; Zheng et al., 2021). While attempts have been made to explore the breaching mechanisms of moraine lake outburst floods, triggered by ice or debris falls, strong earthquake shaking, internal piping, or overtopping waves that exceed the shear resistance of the dam (Emmer and Vilímek, 2013; Richardson and Reynolds, 2000), the understanding of the complex and unclear mechanisms of ice dam lake outburst floods remains a challenge (Werder et al., 2010), making a prediction using complex modelling currently impossible. Therefore, there is an urgent need for simplified approaches to GLOF prediction to mitigate downstream impacts.

Despite the uncertainty related to the detail of GLOF initiation, sudden glacier advances during surge cycles have a prominent role in the formation of ice-dammed lakes by creating an ice barrier in the valleys, particularly at narrow valley floor sections and at confluences (Bazai et al., 2021; Bhambri et al., 2019), damming minor and major rivers. Glacier surges are the main

https://doi.org/10.5194/egusphere-2024-565
Preprint. Discussion started: 21 March 2024

agents related to the formation of ice-dammed lakes in the Swiss Alps (Haeberli, 1983), Northern Norway (Xu et al., 2015), Argentinian Patagonia (Vandekerkhove, 2021), Alaska (Trabant et al., 2003), Karakorum, and in the Pamir (Bazai et al., 2021; Hewitt and Liu, 2010) and Tianshan regions (Ng, 2007; Shangguan et al., 2017). Recent studies reveal that the draining processes of ice-dammed lakes potentially involve subglacial breaching, overspill, rapid ice mass instability, and slow deformation of subglacial cavities (Björnsson, 2003; Haemmig et al., 2014; Round et al., 2017). Several attempts have been made to explore the drainage behaviour of ice-dammed lake outburst floods (Hewitt and Liu, 2010). However, due to the remoteness, danger, and inhospitable terrain where such lakes can be found, real-time data are few, and significant gaps remain in our knowledge of these processes.

In the Karakorum, ice-dammed lakes are found in five major valleys, three of which are densely populated and highly vulnerable to unexpected GLOF events. Recent advances in understanding have been made (Bazai et al., 2021) concerning the formation of episodic ice-dammed lakes, which, due to ice mass transfer variations, are linked to the changes in the glacier surface velocity and fluctuations in the crevasse density during the surge cycle (Rea and Evans, 2011; Sharp, 1985). Despite these advancements in knowledge, globally, the techniques for measuring and estimating lake volume (the volume of the lake before an outburst), the critical depth (for GLOF release), and timely prediction of ice-dammed lakes remain largely unexplored and unidentified (Round et al., 2017; Shangguan et al., 2016; Steiner et al., 2018). Very limited ice-dammed lake volume data are available. Still, these ice-dam lake volumes were measured either while the lake was empty (after the GLOF events) or partially filled and thus shallow (Round et al., 2017; Shangguan et al., 2016; Steiner et al., 2018). The downstream threat from those lakes is extremely high, while their full lake volumes are unknown. To measure the flood volume and flood magnitude for a deep and potentially full lake, the lake volume measurement is recognized as a critical variable that needs to be accurately calculated or at least well-estimated (Bazai et al., 2021; Bazai et al., 2022). An accurate estimate of lake volume will also help explore the timing, triggering depth of the lake, and frequency of ice-dammed lake outburst floods in relation to surge cycles. Timing information can be approximated by correlating glacier velocities and GLOF occurrences (Bazai et al., 2021; Bazai et al., 2022). The current research focuses of Bazai and colleagues aims to leverage historical records, regular field investigations, and remote sensing techniques to develop a comprehensive understanding, which should lead to better prediction of GLOFs through modelling dam failure mechanisms. Herein, the primary objective is to enhance predictive capabilities regarding GLOF event timing by refining empirical lake volume estimation and identifying critical depths for future risk reduction.

2. Methodology:

2.1. Data acquisition

The identification and detection of the Shishper, Khurdopin, and Kyager ice-dammed lakes was accomplished using all available open and commercial satellite imagery sources from 1970 to 2022. The datasets include 590 images of Landsat 2-5, 7-9 and 45 images from Sentinel-2, downloaded from the United States Geological Survey (USGS) website

https://doi.org/10.5194/egusphere-2024-565
Preprint. Discussion started: 21 March 2024

(http://earthexplorer.usgs.gov/) (Table S1). The commercial high-resolution images consisted of 35 images from Gaofen-1 (GF-1) and Gaofen-2 (GF-2), 11 images from SPOT-6 and SPOT-7 and five images from Global Planet (https://data.cresda.cn/#/2dMap, https://earth.esa.int/eogateway and https://www.planet.com/products/planet-imagery, respectively). The following DEM datasets have been used for measuring lake volume, depth and dam height: the Advanced Spaceborne Thermal Emission and Reflection Radiometer (ASTER) and the Phased Array type L-band Synthetic Aperture Radar (PALSAR)-DEM data scenes from the National Aeronautics and Space Administration (NASA) Earth Science Data Center website (https://search.earthdata.nasa.gov/). KH-9 and Shuttle Radar Topography Mission (SRTM) data were downloaded from http://earthexplorer.usgs.gov/ (Table S2). For more precise and high-resolution data, a field survey of the Shishper and Khurdopin glacier lakes was conducted in 2018, 2019, 2021, and 2022 and used Unmanned Aerial Vehicles (UAV) to determine annual lake extents, lake depths, glacier heights, and thickness, termini positions, and glacier surface displacements. The glacier outlines were obtained from the Randolph Glacier Inventory (RGI 6.0) (Consortium, 2017) and modified according to surge movements with time (https://www.planet.com/products/planet-imagery/).

2.2. Glacier Lake mapping and glacier surface velocity

Satellite imagery had a spatial resolution of 0.8 to 30 m (Table S1). The images were selected based on the visibility of the glacier surface and lake areas, and overall, 23 ice-dammed lakes from eight surge events were identified through optical images related to the Khurdopin, Kyager, and Shishper glaciers (Table 1). The presence of lakes was determined based on the Normalized Difference Water Index (NDWI) (McFeeters, 1996), and the outlines of all 23 lakes were digitized manually using Landsat false-color composites (near-infrared, red, and green bands) to distinguish water bodies from other objects (Huggel et al., 2002). The extent of six lakes from Shishper and Khurdopin that occurred after 2017 were obtained in the field using GPS (G639; Accuracy: Single: 1 ~ 3m; SBAS: 0.6m) survey points along the lake shorelines (Fig.1a-d), as well as from Unmanned Aerial Vehicle (UAV) generated Digital Surface Models (DSMs). Field trips were conducted for Khurdopin in 2017 and 2018 and for Shishper in 2019, 2021 and 2022. Alternatively, high-resolution satellite imagery from Planet (3 m) and GF-1 and 2 (0.8 m to 4 m resolution, respectively) and SPOT-6 and SPOT-7 (1.5 m) were used to extract the lake boundaries. The use of high-resolution imagery aims to obtain accurate lake surface levels, and the latter is used for measuring volume and lake depth. The coupled lake extent and polygon help reduce the uncertainty of the lake extent obtained for Landsat 2-5 images. The above method was used to extract the extent of the previous lakes of Khurdopin and Kyager glacier, previously published (Bazai et al., 2021; Bazai et al., 2022), which data are incorporated into the current analysis, and the same method was used to extract the extent of Shishper lakes. These lake polygons and extents were further used to measure lake volume and depth mediated by field derived lake levels as appropriate (Bazai et al., 2022).

https://doi.org/10.5194/egusphere-2024-565
Preprint. Discussion started: 21 March 2024

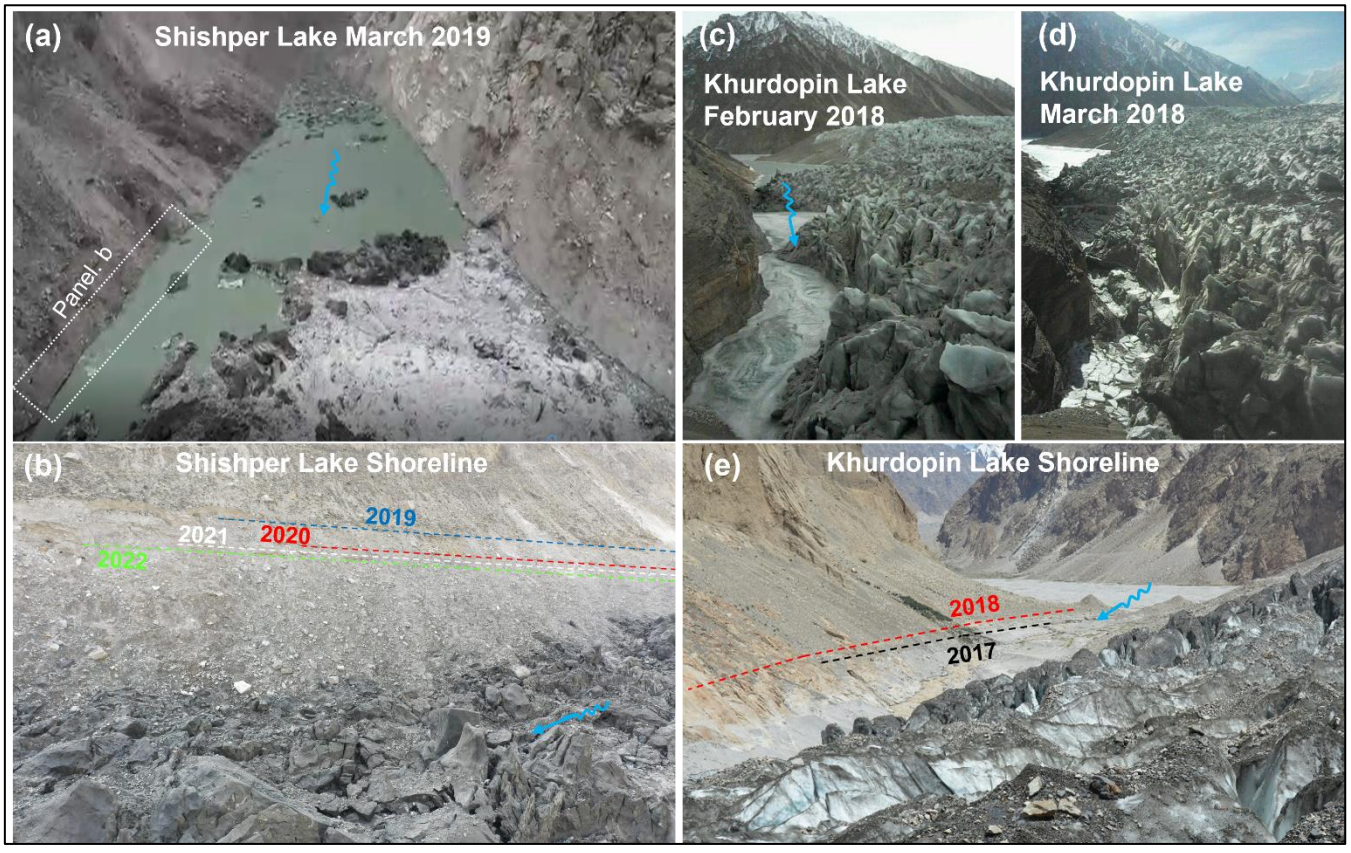

Fig. 01 Shishper and Khurdopin glacial lake view in the field. a) Oblique view from a helicopter in 2019 (image captured in March 2019 during lake monitoring (Image by Gilgit-Baltistan Disaster Management Authority (GBDMA)); b) Shishper shoreline elevations of four lakes that outburst in the given years (image captured in June 2022); c and d are the regular monitoring views of the lake in the field: e) are the lake elevations in the given years. The Khurdopin Lake elevations were identified in the field in April 2018.

The surface velocities of the Khurdopin, Shishper, and Kyager glaciers from 1990 to 2022, highlighting the quiescent and surge phases, were obtained from published data (Bazai et al., 2021; Bazai et al., 2022) using image-to-image correlation open-source software COSI-Corr (Leprince et al., 2012; Leprince et al., 2007). The software effectively assesses the glacier surface velocity (Leprince et al., 2012; Steiner et al., 2018). Utilizing a displacement calculation, this technique was used to co-register and correlate surface features (Bazai et al., 2021; Steiner et al., 2018). The surface velocity and overall movement during the surge were monitored by observing changes in the GPS-registered glacier front positions every three months from March 2019 and measured for three years for the Shishper glacier in the field. When coupled with COSI-Corr measure velocities, these latter procedures gave precise results. The velocity estimation procedure generally yields an accuracy of ¼ of a pixel (Sattar et al., 2019). We estimated velocity root-mean-square errors (RMSE) to justify the image processing accuracy.

https://doi.org/10.5194/egusphere-2024-565
Preprint. Discussion started: 21 March 2024

The Shishper, Khurdopin and Kyager glaciers are surge-type glaciers (Copland et al., 2011; Hewitt, 1998). Since 1972, eight surge events have been occurred from Khurdopin (three surges), Kyager (three surges), and Shishper (two surges) (Table 1) at an interval of 17–20 years for three glaciers. The Landsat 2-4 images from 1970 to 1990 have errors in the selected glacier area. Therefore, the initial surges for Khurdopin and Kyager between 1970 and 1989 were not considered for estimating the annual velocity. Orthorectified Landsat scenes from TM to OLI–2 and sentinel 2 were used to estimate the yearly and event-based velocities of all three glaciers from 1989 to 2022 to obtain information about the surge events and glacier front changes. Within this period (1989 to 2022), some satellite images were absent, and for precise results, cloud-free images were chosen each year.

2.3. Field observation and lake volume measurement

Field observations were performed in the Shimshal and Shishper Valley for the Khurdopin glacier in 2017, 2018, and for Shishper in 2019, 2021, and 2022 to investigate glacier surges, glacier front dynamics, and ice-dammed lakes: lake level and lake depth. The latter value is from shoreline elevations and the elevation of the ice dam at its lowest point (Table 1 and Figure 1). Six lakes were regularly monitored: four from the Shishper Glacier and two from the Khurdopin Glacier. 23 GLOF events from eight surge cycles that occurred during the first year of the surge, or following, are presented in Table 1, with lakes resealing after GLOFs. The field data for six events from the Khurdopin and Shishper glaciers helped to reduce the uncertainty and error for the data related to 17 lake extractions through remote sensing techniques noted above. All the previously recorded lakes from Khurdopin and Shishper were drained via single subglacial conduits with stable inlets and varying outlet positions and lengths. As closely as possible, we identified the inlet and outlet positions of the drainage conduits. The inlet position of the conduit in the ice-dammed lake basin is always in the deepest position, an important factor in determining the lake's depth. The lowest ice dam height also tended to be in the vicinity of the conduit. The inlet positions were geolocated in empty lake basins using GPS, and the lake depth was calculated for these locations. From the field survey, we identified the approximate position of conduits from the presence of surface depressions in the glacier. We estimated the curvilinear conduit lengths between the inlet and outlet.

https://doi.org/10.5194/egusphere-2024-565
Preprint. Discussion started: 21 March 2024

Table 1: GLOF and Surge date and Lake volume measurement since 1970 using remote sensing technique. The average surge velocity of each of the 23 GLOFs from eight surge cycles is presented.

No.s	Glacier Name	Date	Sensor	Lake Area km^2	Aster/UAV Lake Volume Estimate (10^6 m^3)	Lake Vol Uncertainty (+/-$10^6 m^3$)	Vol. after [$10^6 m^3$]	Average velocity (m/d)	Date of next clear image after GLOF	Type of drainage Complete (C) Partial (P)	Surge cycle and Resealed GLOF	Surge Duration in months
	Khurdopin	20/08/1977	LM02								1977–1979	May 1977–Aug 1979; 27 Months
1	Khurdopin	15/8/1999						0.33		C	1998-1999	Jan 1995 to Sep 2002; 92 Months
2	Khurdopin	05/30/2000	L5 TM	1.87	186	2.1	x	0.33	08/26/2000	C	Resealed	
	Khurdopin	04/07/2001	LE07	0.295	19.5	1.5	x	0.44	06/26/2001	C	Resealed	
4	Khurdopin	07/15/2002	LE07	0.60	52.1	1.6	2.2	0.87	08/16/2002	P	Resealed	
5	Khurdopin	07/28/2017	LE07	0.180	16.2	1.4	x	1.41	LC 08 08/01/2017	C	2016-2018	June 2006 to Aug 2009: 38 months
6	Khurdopin	03/18/2018	LC08	0.402	19.8	0.9	x	0.53	02/25/2018	C	Resealed	
7	Kyager	08/01/1977	LM02	1.181	40.73	5.8	x		10/14/1977	C	1976-1977	Jan 1975 to Aug 1978; 43 Months
8	Kyager	07/18/1978	LM02	2.17	82.12	15.6	x		06/07/1979	C	Resealed	
9	Kyager	03/08/1997	L5 TM	3.30	127.3	2.9	x	0.4	04/09/1997	C	1994-1996	Jan 1995 to Sep 2002; 92 Months
10	Kyager	09/10/1998	L5 TM	3.32	133.5	3.5	x	0.3	10/11/1998	C	Resealed	
11	Kyager	09/07/1999	L7ETM+	2.19	86.12	1.23	x	0.46	08/17/1999	C	Resealed	
12	Kyager	06/25/2000	L7ETM+	0.91	23.48	1.12	x	0.49	08/03/2000	C	Resealed	
13	Kyager	09/08/2002	L7ETM+	2.93	115.19	1.09	x	1.29	10/09/2002	C	Resealed	
14	Kyager	06/14/2008	L5 TM	1.45	94.95	1.65	x	0.61	23/06/2008	C	Resealed	June 2006 to Aug 2009: 38 months
15	Kyager	07/28/2009	L5 TM	1.39	91.35	1.56	x	0.56	04/08/2009	C	Resealed	
16	Kyager	07/16/2015	L8 OLI	1.56	53.5	0.87	x	1.14	05/08/2015	C	Resealed	Jan 2013 to Aug 2018: 67 months
17	Kyager	07/14/2016	L7ETM+	1.63	45.89	1.49	2.9	0.53	30/07/2016	P	2014-2016	
18	Kyager	07/31/2016	L7ETM+	1.48	44.32	1.23	x	0.38	08/09/2016	C	Resealed	
19	Kyager	08/10/2017	L8 OLI	2.91	113.99	0.73	11.9	0.38	26/08/2017	P	Resealed	
20	Kyager	08/06/2018	L8 OLI	2.38	87.98	0.53	x	0.29	08/29/2018	C	Resealed	
21	Shishper	06/23/2019	L8 OLI	0.37	24.10	2.1	x	0.95	07/13/2019	C	2017-2019	Dec 2018 to June 2022: 41 Months
22	Shishper	05/29/2020	L8 OLI	0.50	24.90	1.5	x	0.46	06/22/2020	C	Resealed	
23	Shishper	05/16/2021	L8 OLI	0.52	25.77	1.4	x	0.29	07/15/2021	C	Resealed	
	Shishper	05/07/2022	L8 OLI	0.41	27.66	1.1	x	0.24	05/10/2022	C	Resealed	

https://doi.org/10.5194/egusphere-2024-565
Preprint. Discussion started: 21 March 2024

In addition, we used a UAV (DJI Mavic 2 Pro) equipped with a high-resolution camera (4000 pixels × 2250 pixels) to obtain multiple aerial photographs with a minimum of 85% image overlap (Entwistle and Heritage, 2017; Entwistle and Heritage, 2019; Tonkin and Midgley, 2016). The UAV flew at a low uniform height (500 m - to reduce the image distortion) to generate high-resolution orthomosaics and DSMs of the glacier lake surfaces, empty lake basins, and glacier termini. The integral of the difference between the elevation of the lake surface and the elevation of the bottom in the extent of the lake obtains the volume. The lake volume data for the glacial lakes of Khurdopin and Kyager were presented previously (Bazai et al., 2021; Bazai et al., 2022), and the same approach was applied to obtain the Shishper glacier lake volume and depth data (Table 1). In addition to UAV data, we utilized data from KH-9 (1974), ASTER (2000-2019), PALSAR-DEM (June 2008), and SRTM (February 2000) for the computation of lake volumes (Table S2). The SRTM DEM without voids serves as the reference dataset, and the vertical uncertainties of the SRTM DEM are reported to be ±10 m (Rodriguez et al., 2006). The corrected DEMs from Karakorum regions were used by Bazai et al. (2021) and Gardelle et al. (2013).

2.4. Geometry of lake basin

Considering that the lake area in satellite images often exhibits a triangular planform (e.g., Fig 1a), we explored the possibility of using a geometric shape to approximate the volume of the lake basin. It is imperative to accurately extract boundary parameters, including lake elevation, length, width, and depth, and this information was manually acquired. Employing NDWI, we identify lake outliers through Landsat false-color composites, which use near-infrared, red, and green bands to distinguish water bodies from other features. We employ standard connected component analysis to (Dillencourt et al., 1992) to manually calculate the area and the perimeter and determine other dimensions of each lake. Initial calculations are pixel-based and later converted to metric units by multiplying pixel counts with their respective pixel sizes. The pixel size for high-resolution images varied from 0.8 to 3m and was cross-validated with Khurdopin and Shishper glacier lakes UAV data having a pixel size of 0.063m as well as with field survey evidence. Trials demonstrated that the known volume of the lakes determined using DEMs of the lake basins once drained could be approximated if the length of the lake from the upstream inlet to the ice-dam face (*Z*) and the breadth of the lake at the ice dam (*C*) are known. Improved estimates are obtained if the lake's depth (*h*) is known at the deepest point close to the dam face, which value can be obtained from a DEM of the drained basin. Alternatively, where a lake is present, this latter parameter can be obtained by plumbing the depth from a boat.

The first consideration was whether the valley sides might be considered to provide a V-shaped lake cross-section. Each lake volume (V) was approximated by an irregular tetrahedron (Fig. 2a left-hand panel) where the depth (*h*) is unknown, but the distance from A to B (*X* in Fig. 2a) and the length C are known values. Assuming the lake surface is an isosceles triangle, and the vertical face at the dam wall is an equilateral triangle, the volume can be obtained from:

$$V = \sqrt{V^2} \quad (1)$$

$$V^2 = \frac{1}{144}\left[Y_1^2D^2\left(Z_2^2 + X^2 + C^2 + E^2 - Y_1^2 - D^2\right) + Y_2^2E^2\left(Y_1^2 + X^2 + C^2 + D^2 - Y - E^2\right) + Z^2C^2\left(Y_1^2 + Y + D^2 + E^2 - Z^2 - C^2\right) - Y_1^2Y_2^2C^2 - Y_2^2Z^2D^2 - Y_1^2Z^2E^2 - C^2D^2E^2\right]$$

https://doi.org/10.5194/egusphere-2024-565
Preprint. Discussion started: 21 March 2024

Where the values for lakeside lengths Y_1 and Y_2, the main length Z, lakeside length D, and lakeside length E are defined in Fig. 2a and obtained from geometry.

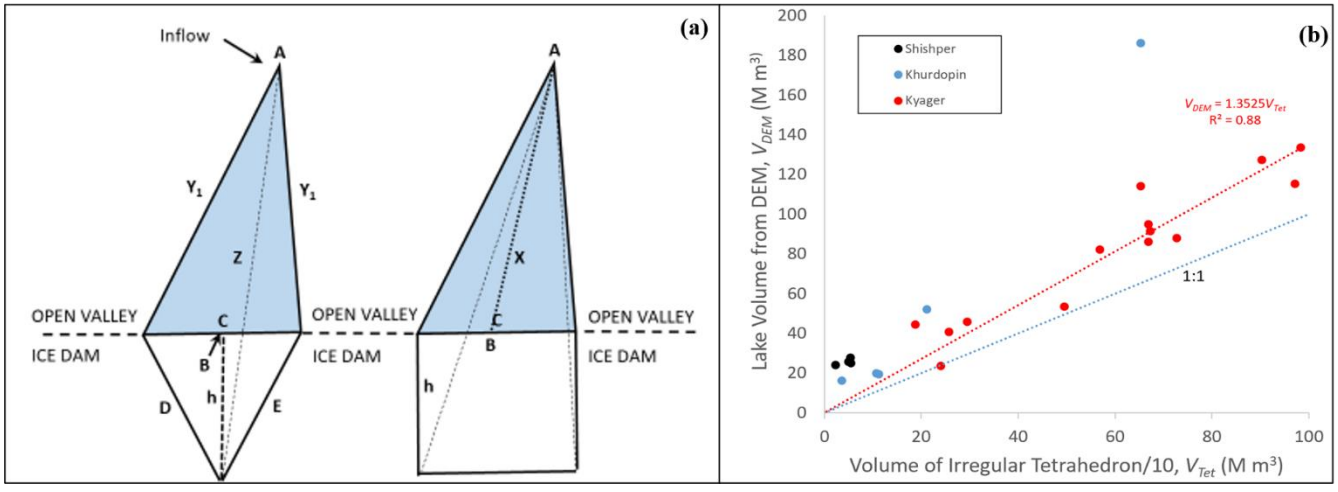

Fig. 02 (a) Definition diagram for calculating the volume of the lakes assuming (left) an irregular tetrahedral shape and (right) an irregular pentahedral shape. The blue shading represents the horizontal surface of the lake, and the white area represents the vertical ice wall. Panel **(b)** Relationship between the volumes of irregular tetrahedrons/10, derived from Eq. 1, and the volumes of the lakes determined using DEMs.

In passing, it can be noted that the volumes of the irregular tetrahedrons in most cases were not dissimilar to the volumes of regular tetrahedrons (*i.e.*, triangular-based pyramids), the equation for which is simple, in contrast to Equation 1. Nevertheless, using equation 1, the volume of the 'tetrahedron' lakes was around 10 times greater than the volume of the lakes determined using the DEMs (Fig. 2b). This result indicates that the actual depth of the lake (*h*) must be much less than that value associated with an equilateral triangle of side length C (Fig. 2a left-hand side).

3. Result:

The relationship between the glacier surge velocity of (Khurdopin, Kyager, and Shishper) and 23 GLOFs is presented in Figure 3a-d and its triggering time or month in the year. In panels a to c, the GLOF occurred after the peak of the glacier surge, and the resealed lake formed while the surge velocity declined. These responses to slowing of the glacier velocity lasted 2-4 years after the surge peak. The relationship between the timing of glacier surges and the timing of GLOFs is shown in Fig. 3d. The three Karakorum glaciers can be used as regional exemplars of surge behavior controlling GLOF occurrence as there is a temporal relationship between the occurrence of periods of glacier surging and the occurrence of GLOFs (Fig. 3a-d). GLOFs occur towards the end of a surge period or immediately afterward; the detail is presented in Table 1. This pattern of behaviour prompted the hypothesis that glacier thickening and thinning during surging might control the development of ice-dammed

https://doi.org/10.5194/egusphere-2024-565
Preprint. Discussion started: 21 March 2024

lakes (Bazai et al., 2022). Lake volumes would increase when the speed of the ice was low such that ice mass would be conserved or increased, and fracturing of the ice would reduce. The corollary pertains to when the ice speed increases, the glacier thins, and the fracturing of the ice mass increases, providing hydraulic drainage conduits.

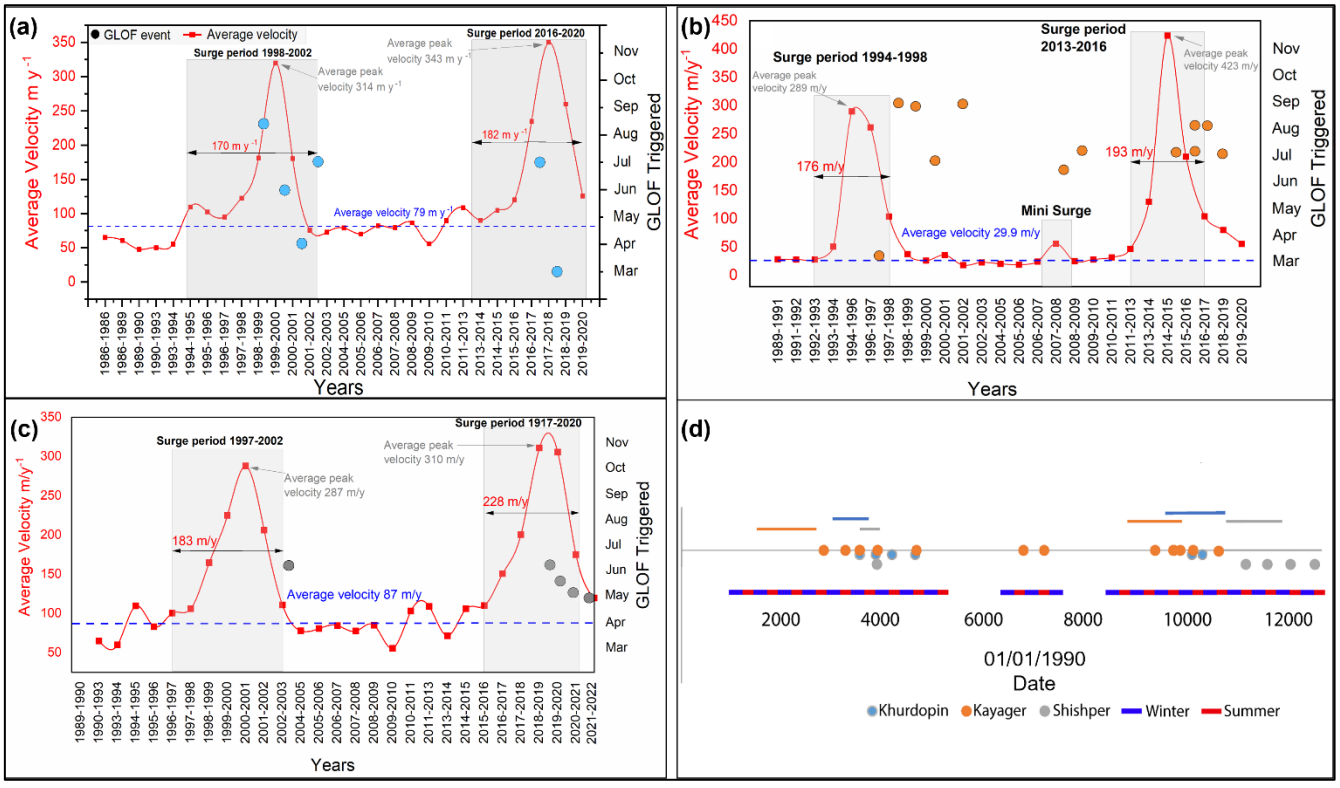

240 **Fig. 03** Relationship between glacier surge and GLOF, with annual glacier velocity analysis during the surge and quiescent phases for three glaciers: (a) Khurdopin, (b) Kyager, and (c) Shishper glacier. GLOFs for these glaciers occurred between the months of March to November. The combined analysis is presented in (d), illustrating the occurrences of GLOFs (dots) in relation to periods of glacier surging (bars). Some points are plotted below the timeline to avoid coincident positions. The blue and red lines show the winter (from October to April) and summer (May to September) seasons in which the GLOF occurred
245 dominantly in the summer months.

As a first attempt to relate glacier behaviour in a predictive sense to lake formation, we sought to determine the resultant lake volume from the prior surge speed. In Fig. 03, the relationship between surge and GLOF was developed using annual velocity data for ease of trend comprehension. However, daily measurements of glacier velocity were conducted to assess its impact on lake volume, given the velocity sensitivity to the triggering time of GLOFs. Consequently, the glacier's daily velocity was
250 specifically recorded on the day when the GLOF was initiated, as detailed in Table 01. Despite a broad data spread, a least-squares regression analysis, with four outliers excluded from the analysis, defines a statistically significant negative power (-1) relationship between surge speed and lake volume (Fig. 4). Raising the glacier surge speed to the power of -2.0 and multiplying by 10 reproduced well the data trend for low glacier surge speeds. Similarly, -0.8 and a -3.0 power functions define the lower and upper limits of the data spreads. These results, although clearly not definitive, were a spur to investigate if there

https://doi.org/10.5194/egusphere-2024-565
Preprint. Discussion started: 21 March 2024

might be a theoretical geometric relationship between the volume of the lake and the control on lake water level exerted by the surge speed. The physical basis for such a relationship is that an increase in surge speed should cause the glacier to thin and fracture after a period of ice thickening and lake volume increase. During surging, the height of the ice barrier impounding the lake would reduce, and fracturing in the ice would increase, both lowering the lake level and reducing the lake surface area. Therefore, surge speed should control lake depth, volume, and potential GLOF volumes.

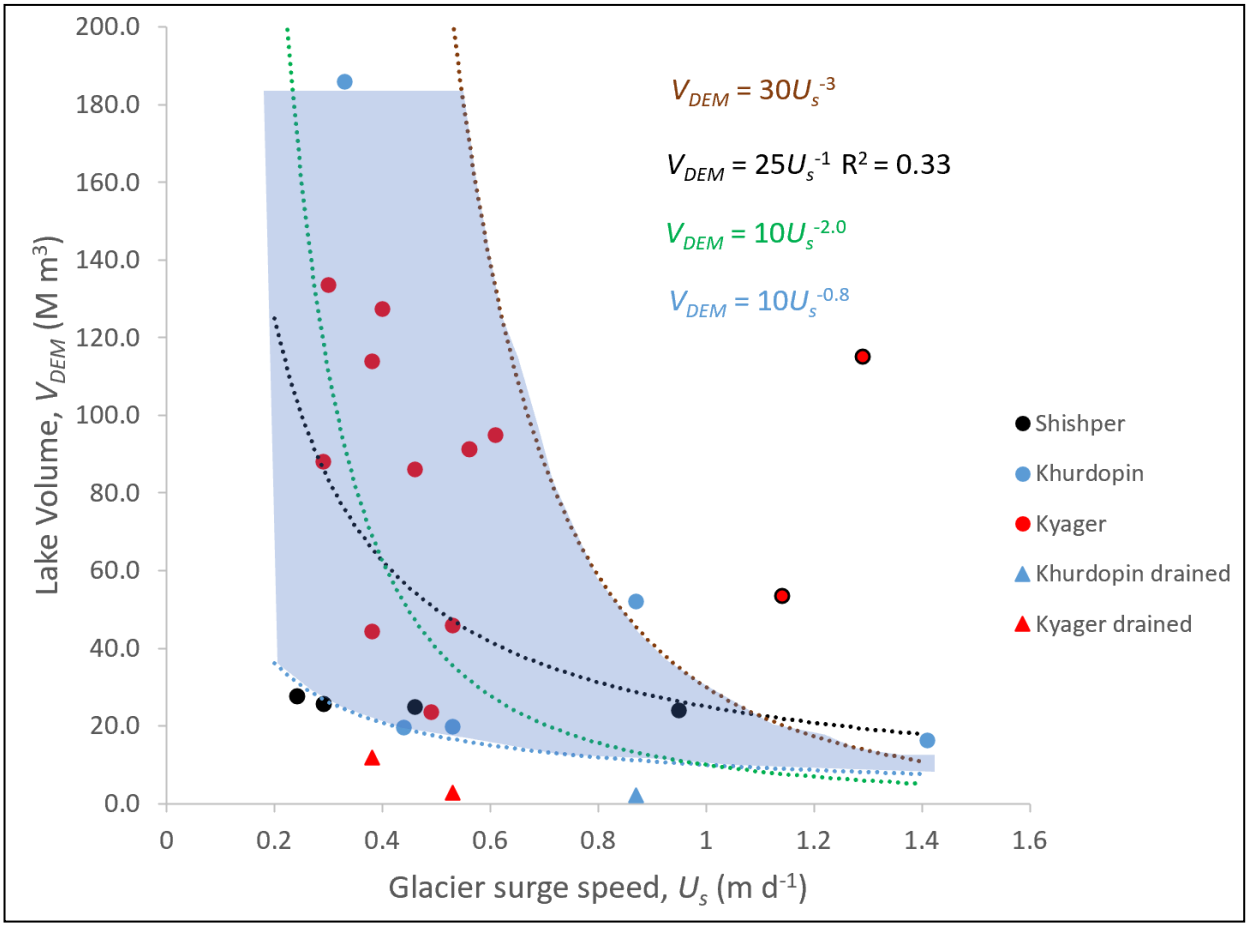

Fig. 04 Variation in glacial lake volume as a function of the glacier surge speed. Data from three glaciers. Most lakes drained completely, but three had residual volumes (triangles). Outliers are shown as black-ringed symbols. A -0.8-power function defines the lower limit to the data spread, whilst a -2.0-power function defines the central tendency of the data trend, and a -3-power function defines the upper limit to the data spread (see text for explanation).

Most of the lakes investigated occur in steep-walled side valleys, the ice dam forming one side of a roughly triangular water surface (Fig. 5a-b). Projecting the valley walls downwards, the geometry of the lake basin can be considered to be either: 1) an irregular tetrahedron, with the lake surface defined as an isosceles triangle (Fig. 5a-b); and the vertical cross-section at the ice dam defined by an equilateral three-sided triangle; or, 2) an irregular pentahedron whereby the vertical cross-section at the ice dam is defined by a quadrilateral (Fig. 2a). In the former case, only the length of the lake (*X*) and the breadth of the lake

https://doi.org/10.5194/egusphere-2024-565
Preprint. Discussion started: 21 March 2024

(*C*) at the ice dam are needed to estimate the lake volume, whereas for the second case, the depth (*h*) of the lake at the ice dam is required as well. The values for *X* and *C* are obtained from remote sensing imagery of the lake surface. Before a GLOF, the depth *h* can be obtained by deploying a plumb-line or echo-sounder in the lake or estimated through a topographic survey of the bounding slopes. Subsequent to GLOF drainage, *h* can be measured from a DEM or field survey. Assuming an irregular tetrahedron (Equation 1) implies the valley walls form a V-shaped cross-section to the lake at the ice dam face. In contrast, assuming an irregular pentahedron implies the valley walls form a square-shaped section, which is more akin to typical U-shaped glacial valleys.

Given the idealized geometric properties of the water mass, and assuming *C* and *X* vary little in contrast to *h*, the lake's volume increases as a function of h^3 (tetrahedron) or h^2 (pentahedron). Given the assumption that depth reduces as surge speed increases provides an explanation for the potential -2 to -3 power function relationships between surge speeds and lake volumes. For example, concerning a tetrahedron, assuming the equilateral geometry is maintained as water depth (*h*) in the lake increases, then, considering Pythagoras' theorem, the volume of the lake increases as the cube of the depth and by corollary as the -3 power of the surge speed. This later function is shown in Fig. 4, and the trend closely defines the upper limit of the empirical data, whilst the -2 relationship, which should pertain to pentahedral volumes, follows the approximate trend of the central tendency of the data spread. Thus, the geometrical properties assumed in the analysis delimit both an upper limit to the relationship between surge velocity and lake volume as well as the main trend.

The appropriateness of assuming geometric shapes for the lake volume was checked by comparing the calculated geometric volumes with the measured DEM lake volumes. Utilizing Eq. 1 and only the values *X* and *C*, the volume of the 'tetrahedron' lakes was around 10 times greater than the volume of the lakes determined using the DEMs (Fig. 2a). This result indicates that the actual depth of the lake (*h*) must be much less than that value associated with an equilateral triangle of side length *C*. Nevertheless, this procedure provides a means to estimate lake volume from plan-view data alone.

https://doi.org/10.5194/egusphere-2024-565
Preprint. Discussion started: 21 March 2024

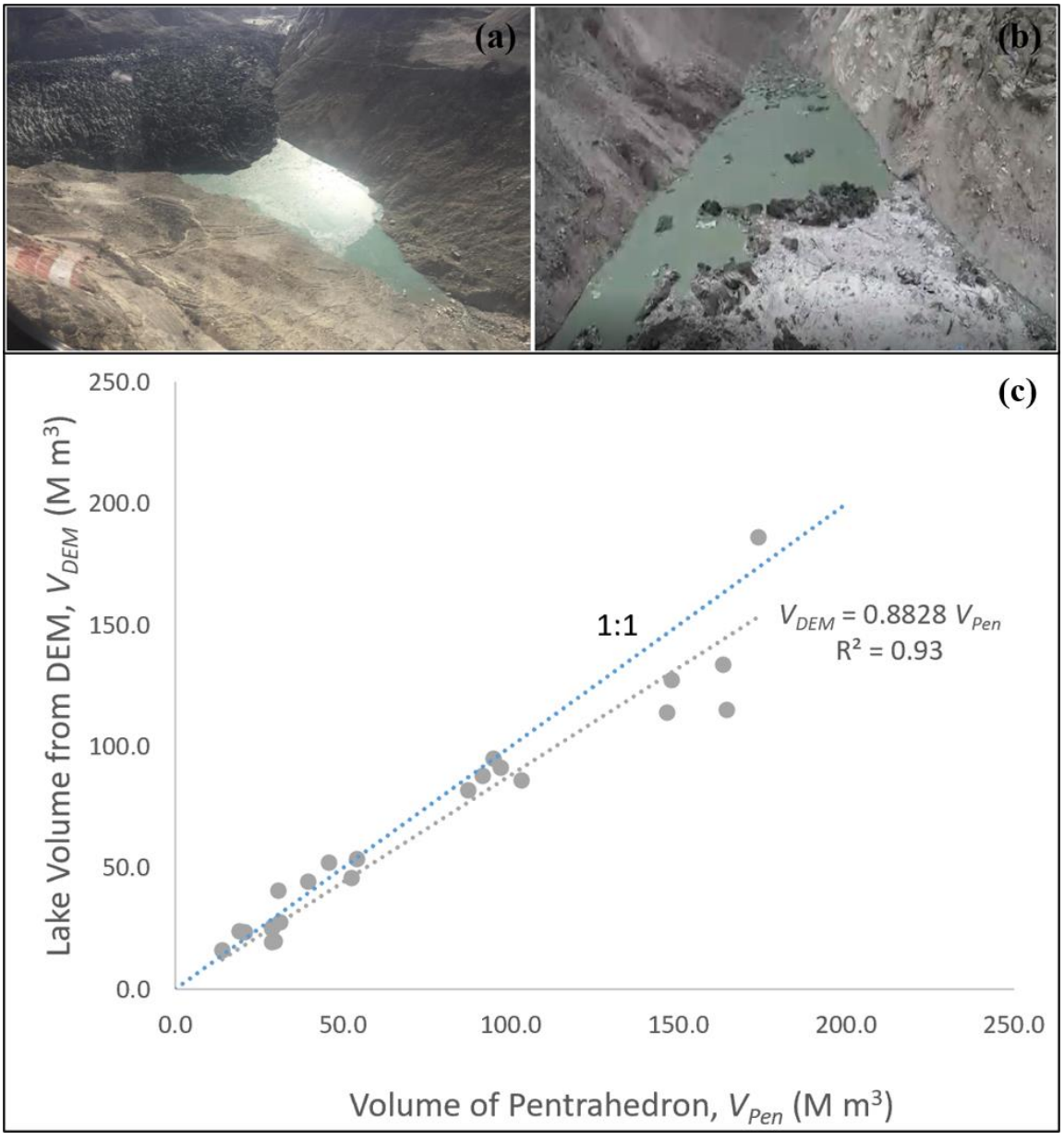

Fig. 05: Examples of Shishper glacial-dammed lakes exhibiting roughly triangular surface 2D shapes and overall pyramidal-shaped volumes (see Fig. 2a); (a) oblique aerial view towards the ice dam; (b) oblique aerial view from the ice dam axially up the impounded valley (image captured in March 2019 during lake monitoring (Image by (Image by Gilgit-Baltistan Disaster
295 Management Authority (GBDMA)). Panel (c) Relationship between the volumes of irregular tetrahedrons/10, derived from Eq. 1, and the volumes of the lakes determined using DEMs.

In contrast to the assumption of a tetrahedron, improving lake volume estimates were obtained considering the measured DEM-derived values of *h* along with the values of *X* and *C*. Once again, assuming an irregular tetrahedron as in Fig. 2a, the analysis demonstrated that the tetrahedral lake volume was roughly half that of the DEM volume (not illustrated). Rather, considering

https://doi.org/10.5194/egusphere-2024-565
Preprint. Discussion started: 21 March 2024

the valley-cross section to be U-shaped (roughly quadrilateral) rather than V-shaped means that doubling the area of the triangular dam face section to form a quadrilateral gives a lake volume defined as an irregular pentahedron (square-based pyramid) (Fig. 2a right-hand side) in contrast to an irregular tetrahedron (Fig. 2a left-hand side). The volume of an irregular pentahedron is:

$$V = \frac{1}{3}(C\ h)X \quad (2)$$

which is more amenable to solving than Equation 1.

The relationship shown in Fig. 5c is preferable to that shown in Fig. 2a as it lies close to the 1:1 relationship between V_{Pen} and V_{DEM} but requires knowledge of the parameters as height or depth: *h*, length; *X*, and width; *C*. In contrast, the less exact relationship in Fig. 2a requires only *X* and *C*. If assuming a rectangular base to the pentahedron exactly matched the DEM volume, then the coefficient value would be unity. Thus, the coefficient of 0.8986 reflects the deviation of the cross-sectional shape of the lake at the dam face from a rectangle. Note that the relationships between both determinations of lake volume progressively deviate from a 1:1 relationship as lake volume increases. This trend might indicate that larger lakes are less well-defined as tetrahedrons or pentahedrons as the volumes increase.

3.1. Predicting the Timing of GLOF Events

The timing of a GLOF remains difficult to determine, but the main driver is the critical depth. The critical depth is that depth that exerts sufficient pressure at the ice dam wall to induce completed connectivity within the sub-glacial GLOF drainage conduit. For the cases of the glacial lakes (Shishper, Khurdopin, and Kyager), the glacial lake depths (*h*) have been normalized by dividing by the minimum value of the ice dam height to give values (*n'*) that range between 0 for a fully-drained lake to a hypothetic value of 1 if the lake level reached the height of the ice barrier. At the approximate time of GLOF occurrence, the resultant values of *n'* range between 0.32 and 0.95 (Fig. 6a-c). Most GLOFs occur for a range of *n'* values between 0.61 and 0.95 (Fig. 6d). Thus, *n'* = 0.60 can be regarded as a warning level value with the risk of a GLOF occurring imminently increasing as *n*' approaches unity.

As the water pressure (*P*) at the dam face increases linearly with water depth in each lake, any variation in the pressure with *n'* that deviates from the linear trend reflects changes in the height of the ice dam (Fig. 6d). Thus, for example, the values of pressure for the Shishper lakes around an *n'* value of 0.8 reflect greater overall ice dam heights in contrast to the Kyager lakes for similar values of *n'*. The two values of low pressure for *n'* < 0.6 reflect low ice dam heights and presumably low structural integrity within the ice mass, allowing ready conduit development. Low values of *n'* (< 0.6) likely are associated with shallow lakes of low hazard potential. Overall, the Kyager data (Fig. 6d) indicate that a minimum water pressure of around 500 kPa should be regarded as a threshold for general concern for GLOF occurrence in the region.

https://doi.org/10.5194/egusphere-2024-565
Preprint. Discussion started: 21 March 2024

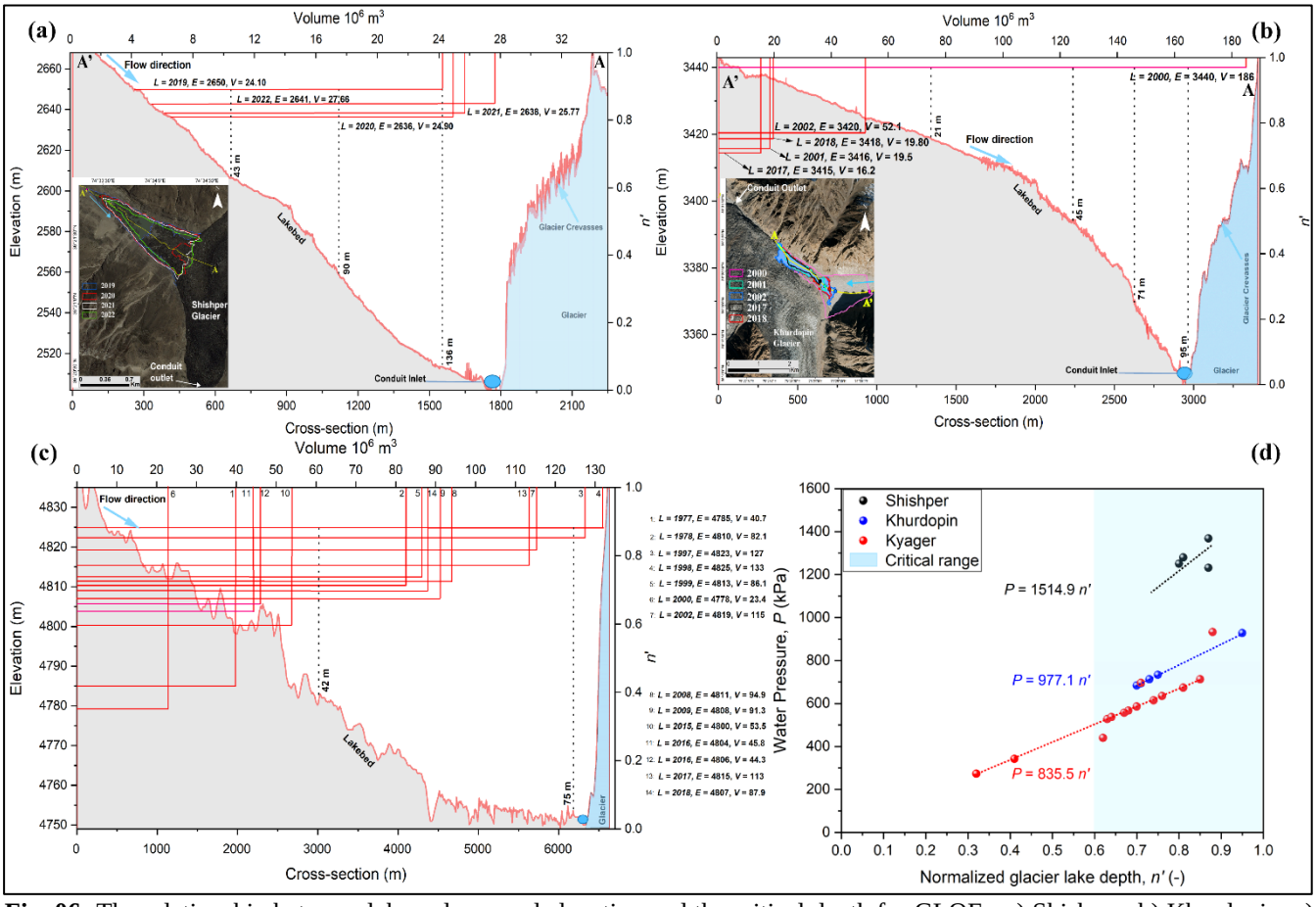

Fig. 06: The relationship between lake volume and elevation and the critical depth for GLOFs. a) Shishper; b) Khurdopin; c) Kyager; d) Water pressure at dam face as a function of *n*'. The cross sections are denoted by (A' and A). The date of each lake flood event is shown as L, E is the lake's elevation, and *V* is the lake volume. The straight, solid red lines relate specific lake elevations to volumes. The UAV photographs captured in the field were used for panel a, and the images captured by the GF-2 were used for panel b.

4. Discussion:

Although predictive models related to ice-dam lake development and subsequent GLOF risk would best be based on modelling the physics of the systems, the controlling parameters are numerous and complex. For example, the mechanisms of glacial sliding, over-burden pressure, tensile and driving stresses require consideration, as do flexure and ice fracture mechanics, thermal erosion, and water pressure, amongst other controls (Carrivick et al., 2020). Few of these controls are well-understood, and, importantly, even where there is an adequate theory, the field data required to inform modelling are absent for specific potential GLOF locations. Consequently, there is an urgent need for simpler methods to predict the likely volume of ice-dammed lakes and the probable triggering water levels that lead to GLOFs. Given that requirement, it is acknowledged that

https://doi.org/10.5194/egusphere-2024-565
Preprint. Discussion started: 21 March 2024

the relationships proposed herein are empirical and apply specifically to glaciers within the Karakorum region. However, there is no reason to suppose that similar functions based on geometric considerations and critical depth (Zhao et al., 2017) might not be developed elsewhere, including for moraine-dammed lakes (Yao et al., 2010). Below, the approach is explored for glacially dammed lakes worldwide.

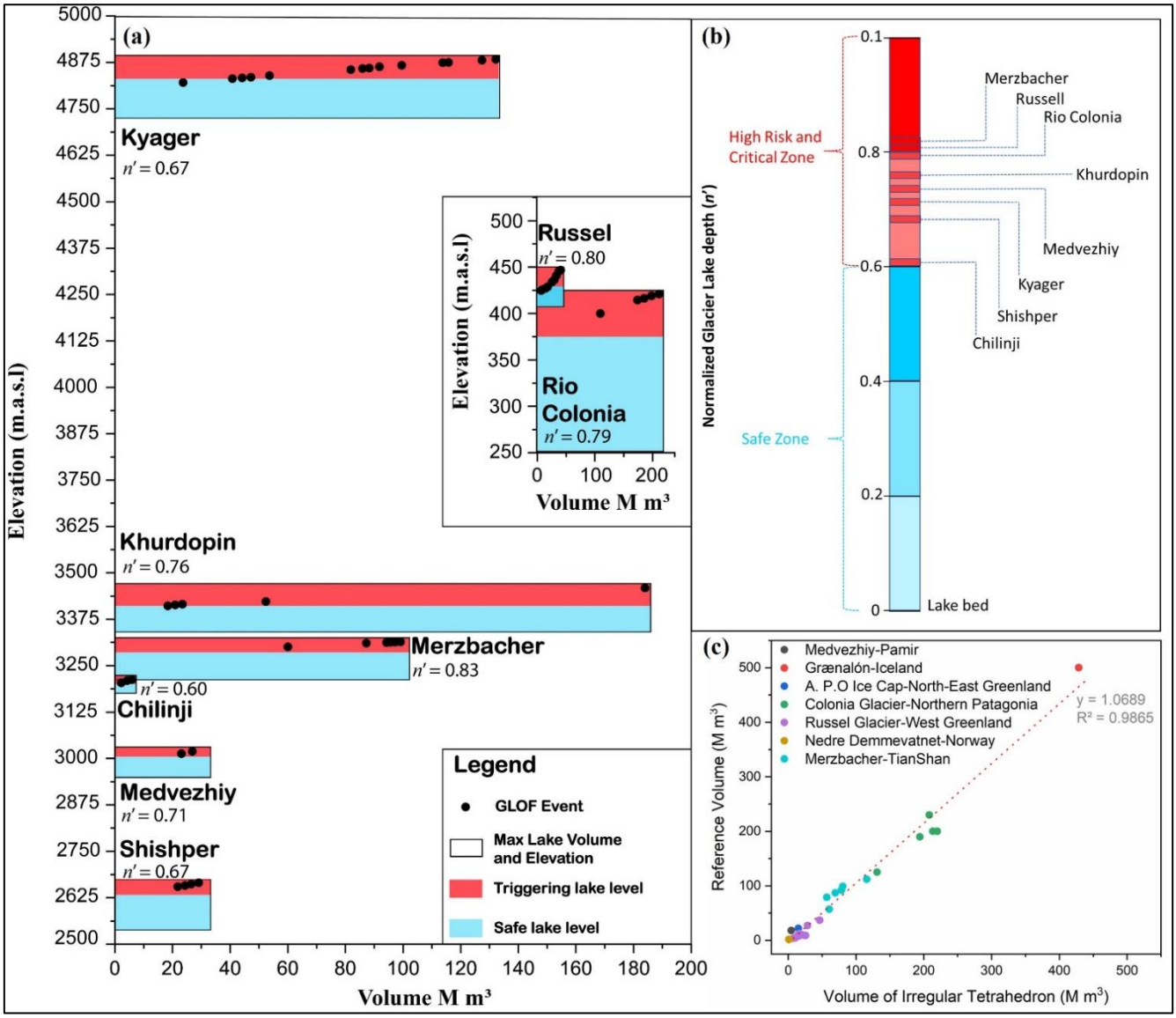

Fig. 07: (a) Represents the maximum volume level of ice-dammed glacier lakes that experience outbursts based on specific volume and elevation criteria. In this representation, the red signifies each lake's triggering level, depth, or zone, where all GLOF events were initiated. Among these lakes, n' values represent the non-dimensional relationship between lake depth and glacier height; panels **(b)** illustrate each lake's normalized critical lake depth and the high-risk and critical zones for Glacial Lake Outburst Floods (GLOFs). It also highlights the high-risk and critical zones for each lake, where values exceeding n' 0.6

https://doi.org/10.5194/egusphere-2024-565
Preprint. Discussion started: 21 March 2024

indicate a critical threshold for the potential occurrence of an ice-dammed lake outburst flood. Panel **(c)** shows the relationship between the referenced volume and measured volume through a geometric approach to the location of glaciers presented in Fig. S1.

Glacially dammed lakes worldwide exhibit consistent behavior in terms of lake formation, filling, and volume gain in response to low glacier velocity (Bazai et al., 2021). Additionally, specific pressure, volume, and critical lake depth values for initiating outburst floods are evident (see Figure 6). Building upon the information presented in Figure 6 for the Karakorum, Figure 7, based on 50 GLOF events from glacial dammed lakes, offers a depiction of the conditions under which glacier lake volume measurements are successfully estimated with high accuracy. Among the 50 GLOF events, 27 examples are given from Pamir, Tianshan, Greenland, and northern Patagonia (see Figure 7a-c). These relevant data are limited, often with only estimates or measurements of lake volume available. Figures 7a and b serve as key components and summaries for this discussion, identifying the lake volumes, elevations, and the critical depth values for GLOF outbursts. The measured lake volumes and the related water surface elevations are shown in Fig. 7a, together with critical depth values (n'). Critical depth values (n') exceed 0.60 in all cases of GLOFs (Fig. 7b), from which we infer that a safe lake level can be defined as ≤ 0.60, and the trigger level is ≥ 0.60. Values of values $n' <$ were associated only with slow, non-catastrophic, lake drainage. Therefore, in the case of future ice-dammed lakes, values of critical depth (n') exceeding 0.60 should be a cause for concern and would serve as a warning level. The geometric procedure outlined herein to estimate lake volume produced an excellent correlation with measured lake volumes (R^2 value of 0.986; Fig. 7c). These findings suggest that future exploration should concentrate on specific volume and depth parameters to determine critical thresholds associated with depth, elevation, or volume for future predictive purposes.

Estimating the volume of an undrained ice-dammed lake from a field survey is dangerous due to floating ice (Fig. 05b), rugged terrain, and sudden drawdowns. The utilization of DEM measurements for lake volume estimation may also introduce high uncertainties or errors due to the difficulty in defining the lake depths (Carrivick et al., 2020; Emmer, 2018). However, for rapid response or mitigation policy purposes, the empirical model (Eq. 1) used in the current study proves to be quite efficient when applied to measure the lake volume before a GLOF.

Understanding glacier surges, lake formation, and the interactions between lakes and glaciers is crucial for advancing knowledge and developing empirical or numerical GLOF models in mountainous regions (Carrivick et al., 2020; Quincey and Luckman, 2014). In this study, the glacier and lake interactions and their relationship have been explored, and their effect on lake volume and draining processes has been examined. Glacier surge speed is routinely determined using remote-sensing imagery (Paul, 2015), as is lake surface area (Quincey and Luckman, 2014). Thus, remote sensing provides a means to develop images similar to Fig. 4 for specific locations around the globe where ice-dammed lakes form due to glacier surging. Although the data within Fig. 4 are scattered, a negative relationship between surge velocity and lake volume is strongly implied. Specifically, data points scatter around a median trend according to a theoretical -2 power function. Most values fall below a theoretical -3 power function (Fig. 4). Clearly, more data points within Fig. 4 would be desirable. Although GLOFs cannot be predicted from this approach, the likely volume of water that might be released catastrophically can be determined. For sites

https://doi.org/10.5194/egusphere-2024-565
Preprint. Discussion started: 21 March 2024

that are deemed to pose a threat to human life and infrastructure, once the lake volume is better constrained, either through DEM analysis or geometric considerations, the value of *n'* for any specific lake provides a ready indicator of the probability of an imminent GLOF. In contrast to the lower trend for water pressures associated with the Kyager lakes, the higher water pressures required to cause the Khurdopin and Shishper lakes to empty may reflect greater structural integrity, possibly related to a greater downstream extent of the glacier dams. These structural issues can be examined in the future. Still, at this stage, if *n'* exceeds 0.6, an initial general warning could be issued to communities downstream of the ice dam. In principle, the estimated volume of a potential GLOF can then be routed downstream using standard hydrodynamic flood routing procedures to determine the timing, depth, and extent of flooding at locations where inundation is forecast. Thus, the severity of the likely impact on humankind can be determined, and specific warning times can be derived from the rate of travel of the GLOFs. These results represent a step forward from the observations made by Carrivick et al. (2020), who proposed the exploration of the interaction between lake water and glaciers to understand the lake formation process and identify lake depth, level, and volume. Based on this understanding, empirical models can be generated to predict GLOFs in a timely manner. The current study offers a comprehensive explanation and advanced knowledge building upon the findings of Carrivick et al. (2020). The study revealed that glacier surge and GLOF development relationship indicates that glacier dynamics control lake volume. Furthermore, the study explores the lake-draining process and identifies the relative depth above which an ice-dammed lake's sudden draining may occur. Future research should further investigate the range of *n'* values and the nature of ice-failure mechanisms connecting lake drawdown and GLOF progression.

5. Conclusion:

The hazards associated with glacier lake outburst floods (GLOFs) in cryospheric regions are increasing worldwide in response to climate change, posing a significant threat to inhabitants in densely populated areas, particularly in the Himalayan Karakoram and Hindu Kush regions. Year on year there is a rise in human casualties and losses to residences, infrastructure, the energy sector, and local and international trade. Despite the escalating risk, the understanding of these hazards remains limited. It is imperative to determine the causes of these hazards, make timely predictions, and formulate new mitigation policies to minimize losses. This research identified the critical depth, lake volume, pressure, and elevation of ice-dammed lakes worldwide associated with GLOFs. An inverse relationship between lake volume and glacier surge speed was observed, indicating that surge speed controls lake depth, volume, and potential GLOF volumes. Comparing surveyed lake volumes with geometric estimates for 23 GLOF events from the Karakoram and 27 events from around the world, a linear regression (R^2 = 0.95) demonstrated that geometric estimates can be robust in the absence of detailed field or remote-sensing surveys. A GLOF will likely occur when the lake's non-dimensional depth (*n'*) exceeds 0.60, corresponding to a typical water pressure on the dam face of 510 kPa.

Competing interests

The authors declare no conflict of interest.

https://doi.org/10.5194/egusphere-2024-565
Preprint. Discussion started: 21 March 2024

Acknowledgements

This study was supported by the Second Tibet Plateau Scientific Expedition and Research Program (STEP) (Grant No. 2019QZKK0906) and the National Natural Science Foundation of China（Grant no. 42350410445). Special thanks to the monitoring team of Gilgit-Baltistan Disaster Management Authority (GBDMA), Quaid-i-Azam University, and Karakoram International University for their support and data sharing, and thanks to the Special Research Assistant program of the Chinese Academy of Sciences.

Author Contributions

N.A.B. conceptualized and designed the study and methodology, generated and compiled field data, processed data visualization, and drafted the manuscript. P.A.C. contributed to conceptualization, methodology, interpretation, discussion, review, and editing. P.C. supervised funding acquisition and commented on the paper, and H.W. contributed to compiling the field data. N.A.B., G.T.Z., J.W, D.Z.L, and J.H contributed to remote sensing data analysis.

Supplementary Information

Supplementary information for this paper is available in supplementary material and at https://doi.org/10.1016/j.earscirev.2020.103432 and https://doi.org/10.1016/j.gloplacha.2021.103710.

https://doi.org/10.5194/egusphere-2024-565
Preprint. Discussion started: 21 March 2024

References

Bazai, N. A., Cui, P., Carling, P. A., Wang, H., Hassan, J., Liu, D., Zhang, G., and Jin, W.: Increasing glacial lake outburst flood hazard in response to surge glaciers in the Karakoram, ESRv, 212, 103432, 2021.

Bazai, N. A., Cui, P., Liu, D., Carling, P. A., Wang, H., Zhang, G., Li, Y., and Hassan, J.: Glacier surging controls glacier lake formation and outburst floods: The example of the Khurdopin Glacier, Karakoram, Glob. Planet. Change, 208, 103710, 2022.

Berthier, E. and Brun, F.: Karakoram geodetic glacier mass balances between 2008 and 2016: persistence of the anomaly and influence of a large rock avalanche on Siachen Glacier, J. Glaciol, 65, 494-507, 2019.

Bhambri, R., Bolch, T., Kawishwar, P., Dobhal, D., Srivastava, D., and Pratap, B.: Heterogeneity in glacier response in the upper Shyok valley, northeast Karakoram, The Cryosphere, 7, 1385-1398, 2013.

Bhambri, R., Hewitt, K., Kawishwar, P., Kumar, A., Verma, A., Tiwari, S., and Misra, A.: Ice-dams, outburst floods, and movement heterogeneity of glaciers, Karakoram, Glob. Planet. Change, 180, 100-116, 2019.

Björnsson, H.: Subglacial lakes and jökulhlaups in Iceland, Glob. Planet. Change, 35, 255-271, 2003.

Bolch, T., Pieczonka, T., and Benn, D.: Multi-decadal mass loss of glaciers in the Everest area (Nepal Himalaya) derived from stereo imagery, The Cryosphere, 5, 349-358, 2011.

Bolch, T., Pieczonka, T., Mukherjee, K., and Shea, J. M.: Brief communication: Glaciers in the Hunza catchment (Karakoram) have been nearly in balance since the 1970s, The Cryosphere, 11, 531-539, 2017.

Byers, A. C., Somos-Valenzuela, M., Shugar, D. H., McGrath, D., Chand, M. B., and Avtar, R.: Brief Communication: An Ice-Debris Avalanche in the Nupchu Valley, Kanchenjunga Conservation Area, Eastern Nepal, EGUsphere, 2023, 1-8, 2023.

Carling, P. A.: Freshwater megaflood sedimentation: What can we learn about generic processes?, Earth-Sci. Rev, 125, 87-113, 2013.

Carrivick, J. L. and Tweed, F. S.: A global assessment of the societal impacts of glacier outburst floods, Glob. Planet. Change, 144, 1-16, 2016.

Carrivick, J. L., Tweed, F. S., Sutherland, J. L., and Mallalieu, J.: Toward numerical modeling of interactions between ice-marginal proglacial lakes and glaciers, Front. Earth Sci., 2020. 500, 2020.

Consortium, R.: Randolph glacier inventory–a dataset of global glacier outlines: Version 6.0: technical report, global land ice measurements from space, Colorado, USA, Digital Media, 2017. 2017.

Cook, S. J., Kougkoulos, I., Edwards, L. A., Dortch, J., and Hoffmann, D.: Glacier change and glacial lake outburst flood risk in the Bolivian Andes, The Cryosphere, 10, 2399-2413, 2016.

Copland, L., Sylvestre, T., Bishop, M. P., Shroder, J. F., Seong, Y. B., Owen, L. A., Bush, A., and Kamp, U.: Expanded and recently increased glacier surging in the Karakoram, Arct. Antarct. Alp. Res., 43, 503-516, 2011.

Cui, P., Chen, R., Xiang, L., and Su, F.: Risk analysis of mountain hazards in Tibetan plateau under global warming, Progressus Inquisitiones De Mutatione Climatis, 2, 103-109, 2014.

Cui, P., Su, F., Zou, Q., Chen, N., and Zhang, Y.: Risk assessment and disaster reduction strategies for mountainous and meteorological hazards in Tibetan Plateau, Chin. Sci. Bull., 60, 3067-3077, 2015.

Dehecq, A., Gourmelen, N., Gardner, A. S., Brun, F., Goldberg, D., Nienow, P. W., Berthier, E., Vincent, C., Wagnon, P., and Trouvé, E.: Twenty-first century glacier slowdown driven by mass loss in High Mountain Asia, Nat. Geosci., 12, 22-27, 2019.

Dillencourt, M. B., Samet, H., and Tamminen, M.: A general approach to connected-component labeling for arbitrary image representations, Journal of the ACM (JACM), 39, 253-280, 1992.

Emmer, A.: Glacier retreat and glacial lake outburst floods (GLOFs). In: Oxford Research Encyclopedia of Natural Hazard Science, 2017.

Emmer, A.: GLOFs in the WOS: Bibliometrics, geographies and global trends of research on glacial lake outburst floods (Web of Science, 1979–2016), NHESS, 18, 813, 2018.

Emmer, A. and Vilímek, V.: Lake and breach hazard assessment for moraine-dammed lakes: an example from the Cordillera Blanca (Peru), NHESS, 13, 1551-1565, 2013.

Entwistle, N. and Heritage, G.: An evaluation DEM accuracy acquired using a small unmanned aerial vehicle across a riverine environment, Int. j. new Technol. Res, 3, 43-48, 2017.

Entwistle, N. S. and Heritage, G. L.: Small unmanned aerial model accuracy for photogrammetrical fluvial bathymetric survey, J. Appl. Remote Sens., 13, 014523, 2019.

Farinotti, D., Immerzeel, W. W., de Kok, R. J., Quincey, D. J., and Dehecq, A.: Manifestations and mechanisms of the Karakoram glacier Anomaly, Nat. Geosci, 13, 8-16, 2020.

Frey, H., Machguth, H., Huss, M., Huggel, C., Bajracharya, S., Bolch, T., Kulkarni, A., Linsbauer, A., Salzmann, N., and Stoffel, M.: Estimating the volume of glaciers in the Himalayan–Karakoram region using different methods, The Cryosphere, 8, 2313-2333, 2014.

Gardelle, J., Berthier, E., and Arnaud, Y.: Slight mass gain of Karakoram glaciers in the early twenty-first century, Nat. Geosci, 5, 322-325, 2012.

Gardelle, J., Berthier, E., Arnaud, Y., and Kaab, A.: Region-wide glacier mass balances over the Pamir-Karakoram-Himalaya during 1999-2011 (vol 7, pg 1263, 2013), 2013. 2013.

Haeberli, W.: Frequency and characteristics of glacier floods in the Swiss Alps, Ann. Glaciol., 4, 85-90, 1983.

https://doi.org/10.5194/egusphere-2024-565
Preprint. Discussion started: 21 March 2024

Haemmig, C., Huss, M., Keusen, H., Hess, J., Wegmüller, U., Ao, Z., and Kulubayi, W.: Hazard assessment of glacial lake outburst floods from Kyagar glacier, Karakoram mountains, China, Annals of Glaciology, 55, 34-44, 2014.
Harrison, S., Kargel, J. S., Huggel, C., Reynolds, J., Shugar, D. H., Betts, R. A., Glasser, N., Haritashya, U. K., Klimeš, J., and Reinhardt, L.: Climate change and the global pattern of moraine-dammed glacial lake outburst floods, TC, 12, 2018.
Hewitt, K.: Natural dams and outburst floods of the Karakoram Himalaya, IAHS, 138, 259-269, 1982.
Hewitt, K.: Recent glacier surges in the Karakoram Himalaya, south central Asia, Eos, 78, 46, 1998.
Hewitt, K. and Liu, J.: Ice-dammed lakes and outburst floods, Karakoram Himalaya: historical perspectives on emerging threats, Phys. Geogr., 31, 528-551, 2010.
Huggel, C., KääB, A., Haeberli, W., Teysseire, P., and Paul, F.: Remote sensing based assessment of hazards from glacier lake outbursts: a case study in the Swiss Alps, CaGeJ, 39, 316-330, 2002.
John, Clague, and, Stephen, and Evans: A review of catastrophic drainage of moraine-dammed lakes in British Columbia, QSRv, 2000. 2000.
Kääb, A. and Girod, L.: Brief communication: Rapid∼ 335× 10 6 m 3 bed erosion after detachment of the Sedongpu Glacier (Tibet), The Cryosphere, 17, 2533-2541, 2023.
Kääb, A., Treichler, D., Nuth, C., and Berthier, E.: Brief Communication: Contending estimates of 2003–2008 glacier mass balance over the Pamir–Karakoram–Himalaya, TC, 9, 2015.
Kreutzmann, H.: Habitat conditions and settlement processes in the Hindukush-Karakoram, Petermanns Geogr. Mitt, 138, 337-356, 1994.
Leprince, S., Avouac, J.-P., and Ayoub, F.: Ortho-rectification, coregistration, and subpixel correlation of optical satellite and aerial images. Google Patents, 2012.
Leprince, S., Barbot, S., Ayoub, F., and Avouac, J.-P.: Automatic and precise orthorectification, coregistration, and subpixel correlation of satellite images, application to ground deformation measurements, ITGRS, 45, 1529-1558, 2007.
Mason, K.: Indus floods and Shyok glaciers, Himal. J, 1, 10-29, 1929.
McFeeters, S. K.: The use of the Normalized Difference Water Index (NDWI) in the delineation of open water features, Int. J. Remote Sens., 17, 1425-1432, 1996.
Minora, U., Bocchiola, D., D'Agata, C., Maragno, D., Mayer, C., Lambrecht, A., Mosconi, B., Vuillermoz, E., Senese, A., and Compostella, C.: 2001–2010 glacier changes in the Central Karakoram National Park: a contribution to evaluate the magnitude and rate of the" Karakoram anomaly", The Cryosphere Discussions, 7, 2891-2941, 2013.
Neupane, R., Chen, H., and Cao, C.: Review of moraine dam failure mechanism, Geomatics Nat. Hazards Risk, 10, 1948-1966, 2019.
Ng, F.: Climatic control on the peak discharge of glacier outburst floods, Geophys. Res. Lett., 2007. 2007.
Paul, F.: Revealing glacier flow and surge dynamics from animated satellite image sequences: examples from the Karakoram, The Cryosphere, 9, 2201-2214, 2015.
Quincey, D. and Luckman, A.: Brief Communication: On the magnitude and frequency of Khurdopin glacier surge events, The Cryosphere, 8, 571-574, 2014.
Rea, B. R. and Evans, D. J.: An assessment of surge-induced crevassing and the formation of crevasse squeeze ridges, J. Geophys. Res.: Earth Surf., 116, 2011.
Richardson, S. D. and Reynolds, J. M.: An overview of glacial hazards in the Himalayas, Quat Int, 65, 31-47, 2000.
Rick, B., McGrath, D., McCoy, S., and Armstrong, W.: Unchanged frequency and decreasing magnitude of outbursts from ice-dammed lakes in Alaska, Nat. Commun., 14, 6138, 2023.
Rodriguez, E., Morris, C. S., and Belz, J. E.: A global assessment of the SRTM performance, Photogrammetric Engineering & Remote Sensing, 72, 249-260, 2006.
Round, V., Leinss, S., Huss, M., Haemmig, C., and Hajnsek, I.: Surge dynamics and lake outbursts of Kyagar Glacier, Karakoram, TC, 11, 723-739, 2017.
Sattar, A., Goswami, A., Kulkarni, A. V., and Das, P.: Glacier-Surface Velocity Derived Ice Volume and Retreat Assessment in the Dhauliganga Basin, Central Himalaya – A Remote Sensing and Modeling Based Approach, Front. Earth Sci., 7, 2019.
Shangguan, D., Ding, Y., Liu, S., Xie, Z., Pieczonka, T., Xu, J., and Moldobekov, B.: Quick release of internal water storage in a glacier leads to underestimation of the hazard potential of glacial lake outburst floods from lake merzbacher in central tian shan mountains, Geophys. Res. Lett., 44, 9786-9795, 2017.
Shangguan, D., Liu, S., Ding, Y., Guo, W., Xu, B., Xu, J., and Jiang, Z.: Characterizing the May 2015 Karayaylak Glacier surge in the eastern Pamir Plateau using remote sensing, JGlac, 62, 944-953, 2016.
Sharp, M.: "Crevasse-fill" ridges—a landform type characteristic of surging glaciers?, Geogr. Ann. Ser. A Phys. Geogr., 67, 213-220, 1985.
Steiner, J. F., Kraaijenbrink, P. D., Jiduc, S. G., and Immerzeel, W. W.: Brief communication: The Khurdopin glacier surge revisited-Extreme flow velocities and formation of a dammed lake in 2017, TC, 12, 95-101, 2018.
Stuart-Smith, R., Roe, G., Li, S., and Allen, M.: Increased outburst flood hazard from Lake Palcacocha due to human-induced glacier retreat, Nat. Geosci., 14, 85-90, 2021.
Tonkin, T. N. and Midgley, N. G.: Ground-control networks for image based surface reconstruction: An investigation of optimum survey designs using UAV derived imagery and structure-from-motion photogrammetry, Remote Sens, 8, 786, 2016.

https://doi.org/10.5194/egusphere-2024-565
Preprint. Discussion started: 21 March 2024

Trabant, D. C., March, R., and Thomas, D.: Hubbard Glacier, Alaska: Growing and advancing in spite of global climate change and the 1986 and 2002 Russell Lake outburst floods, US Geological Survey, 907, 786-7100, 2003.

Vandekerkhove, E.: Impact of climate change on the occurrence of late Holocene glacial lake outburst floods in Patagonia: A sediment perspective, 2021. Ghent University, 2021.

Veh, G., Lützow, N., Tamm, J., Luna, L. V., Hugonnet, R., Vogel, K., Geertsema, M., Clague, J. J., and Korup, O.: Less extreme and earlier outbursts of ice-dammed lakes since 1900, Nature, 614, 701-707, 2023.

Werder, M. A., Bauder, A., Funk, M., and Keusen, H. R.: Hazard assessment investigations in connection with the formation of a lake on the tongue of Unterer Grindelwaldgletscher, Bernese Alps, Switzerland, NHESS, 10, 474-479 Vol. 471, 2010.

Xu, M., Bogen, J., Wang, Z., Bønsnes, T. E., and Gytri, S.: Pro-glacial lake sedimentation from jökulhlaups (GLOF), Blåmannsisen, northern Norway, ESPL, 40, 654-665, 2015.

Yao, T., Thompson, L. G., Mosbrugger, V., Zhang, F., Ma, Y., Luo, T., Xu, B., Yang, X., Joswiak, D. R., and Wang, W.: Third pole environment (TPE), Environ. Dev., 3, 52-64, 2012.

Yao, X., Liu, S., and Wei, J.: Reservoir capacity calculation and variation of Moraine-dammed Lakes in the North Himalayas: a case study of Longbasaba Lake, Aata Geographica Sinica, 65, 1381-1390, 2010.

Yong, Nie, Yongwei, Sheng, Qiao, Liu, Linshan, Liu, Shiyin, and Liu: A regional-scale assessment of Himalayan glacial lake changes using satellite observations from 1990 to 2015, Remote Sens. Environ., 2017. 2017.

You, C. and Xu, C.: Himalayan glaciers threatened by frequent wildfires, Nat. Geosci., 15, 956-957, 2022.

Zhang, T., Li, D., East, A. E., Walling, D. E., Lane, S., Overeem, I., Beylich, A. A., Koppes, M., and Lu, X.: Warming-driven erosion and sediment transport in cold regions, Nature Reviews Earth & Environment, 3, 832-851, 2022.

Zhang, X. S., Zhou, Y.C., et al.,: The Researches Of Glacier Lake Outburst Floods Of The Yarkant River In Xinjiang, Sci. China, Ser. B: Chem., 1990. 120-130+132, 1990.

Zhao, T.-y., Yang, M.-y., Walling, D. E., Zhang, F.-b., and Zhang, J.-q.: Using check dam deposits to investigate recent changes in sediment yield in the Loess Plateau, China, Global Planet. Change, 152, 88-98, 2017.

Zheng, G., Allen, S. K., Bao, A., Ballesteros-Cánovas, J. A., Huss, M., Zhang, G., Li, J., Yuan, Y., Jiang, L., and Yu, T.: Increasing risk of glacial lake outburst floods from future Third Pole deglaciation, Nat. Clim. Change, 11, 411-417, 2021.